



HAL
open science

Late Holocene Paleoenvironmental Evolution of Two Coastal Lakes in Mediterranean Chile and Its Implications for Conservation Planning

Isis-Yelena Montes, Andy Banegas-Medina, Nathalie Fagel, Meriam El Ouahabi, Elie Verleyen, Denisse Alvarez, Fernando Torrejón, Sabine Schmidt, Gilles Lepoint, Gustavo Diaz, et al.

► **To cite this version:**

Isis-Yelena Montes, Andy Banegas-Medina, Nathalie Fagel, Meriam El Ouahabi, Elie Verleyen, et al.. Late Holocene Paleoenvironmental Evolution of Two Coastal Lakes in Mediterranean Chile and Its Implications for Conservation Planning. Applied Sciences, 2021, 11, 10.3390/app11083478 . hal-03337094

HAL Id: hal-03337094

<https://hal.science/hal-03337094v1>

Submitted on 7 Sep 2021

HAL is a multi-disciplinary open access archive for the deposit and dissemination of scientific research documents, whether they are published or not. The documents may come from teaching and research institutions in France or abroad, or from public or private research centers.






L'archive ouverte pluridisciplinaire **HAL**, est destinée au dépôt et à la diffusion de documents scientifiques de niveau recherche, publiés ou non, émanant des établissements d'enseignement et de recherche français ou étrangers, des laboratoires publics ou privés.



Distributed under a Creative Commons Attribution - NonCommercial - NoDerivatives 4.0 International License

Article

Late Holocene Paleoenvironmental Evolution of Two Coastal Lakes in Mediterranean Chile and Its Implications for Conservation Planning

Isis-Yelena Montes ^{1,2,*} , Andy Banegas-Medina ^{1,2}, Nathalie Fagel ³, Meriam El Ouahabi ³ , Elie Verleyen ⁴, Denisse Alvarez ^{1,5} , Fernando Torrejón ¹, Sabine Schmidt ⁶ , Gilles Lepoint ⁷, Gustavo Diaz ¹, Pablo Pedreros ¹  and Roberto Urrutia ¹

- ¹ Centre of Environmental Sciences EULA-Chile and CHRIAM Water Research Centre, Department of Aquatic Systems, Faculty of Environmental Sciences, Universidad de Concepción, P.O. Box 160-C Concepción, Chile; bbanegas@udec.cl (A.B.-M.); dealvarezsa@santotomas.cl (D.A.); ftorrejo@udec.cl (F.T.); gusdiaz@udec.cl (G.D.); papedrer@udec.cl (P.P.); rurrutia@udec.cl (R.U.)
- ² Laboratory of Biology, Department of Sciences, Danlí Technological Campus, National Autonomous University of Honduras (UNAH), Pan-American Highway km 95, 13201 Danlí, Honduras
- ³ Departement of Geology, AGES, University of Liège, Liège, Quartier Agora, allée du six Août 14, 4000 Liège, Belgium; nathalie.fagel@uliege.be (N.F.); meriam.elouahabi@uliege.be (M.E.O.)
- ⁴ Laboratory of Protistology and Aquatic Ecology, Department of Biology, Ghent University, Krijgslaan 281-S8, B-9000 Ghent, Belgium; elie.verleyen@ugent.be
- ⁵ Facultad de Ciencias, Universidad Santo Tomás, 4030585 Concepción, Chile
- ⁶ CNRS, Univ. Bordeaux, EPOC, EPHE, UMR 5805, Allée Geoffroy Saint-Hilaire, 33615 Pessac, France; sabine.schmidt@u-bordeaux.fr
- ⁷ Laboratory of Oceanology, Freshwater and Oceanic Science Unit of Research (FOCUS), University of Liège, Quartier Agora, allée du six Août 11, 4000 Liège Liège, Belgium; g.lepoint@uliege.be
- * Correspondence: imontes@udec.cl



Citation: Montes, I.-Y.; Banegas-Medina, A.; Fagel, N.; El Ouahabi, M.; Verleyen, E.; Alvarez, D.; Torrejón, F.; Schmidt, S.; Lepoint, G.; Diaz, G.; et al. Late Holocene Paleoenvironmental Evolution of Two Coastal Lakes in Mediterranean Chile and Its Implications for Conservation Planning. *Appl. Sci.* **2021**, *11*, 3478. <https://doi.org/10.3390/app11083478>

Academic Editor: Jordi Revelles

Received: 23 February 2021

Accepted: 28 March 2021

Published: 13 April 2021

Publisher's Note: MDPI stays neutral with regard to jurisdictional claims in published maps and institutional affiliations.



Copyright: © 2021 by the authors. Licensee MDPI, Basel, Switzerland. This article is an open access article distributed under the terms and conditions of the Creative Commons Attribution (CC BY) license (<https://creativecommons.org/licenses/by/4.0/>).

Abstract: Paleolimnological reconstructions from the mid and high latitudes in the Southern Hemisphere are still relatively scarce. Anthropogenic impacts have evidenced trophic state changes and an increase in cyanobacterial blooms in the lacustrine system of San Pedro de la Paz in the last decades. Here, we reconstructed primary production and sedimentological changes spanning the past 2500 years in two coastal lakes in Mediterranean Chile. A multiproxy approach including sedimentological, biogenic silica, carbon and nitrogen isotopes and fossil pigments analysis in sediment cores was performed in Laguna Grande (LGSP) and Laguna Chica de San Pedro (LCSP). A marked change in the sedimentology of the lakes, likely related to the terrigenous sediment inputs derived by a transition from an arid condition in the mid-Holocene to a more humid condition in the late Holocene that favoured arboreal forest establishment at 100 BC–AD 150. A period of low primary production was identified between 850 to 1050 AC for LCSP, suggesting moist and cold conditions that were possibly related to La Niña events. In recent decades, there have been increases in primary production, probably resulting from anthropogenic disturbances. These likely include the clearance of native vegetation, the introduction of exotic tree species, and urbanisation, which in turn, resulted in nutrient inputs and hence eutrophication. We conclude that an integrated management program for both lakes is urgently needed.

Keywords: lacustrine sediments; algal pigments; multi-proxy; reconstruction; environmental changes

1. Introduction

Lake sediments are archives of past variations in biological communities which respond to environmental and climate change and vary in time and space [1–5]. These changes result from a complex interaction between climate, anthropogenic activities and the characteristic of aquatic systems that imply its study and recording [5–7]. Such records are particularly lacking for the Southern Hemisphere [6–8]. The Mediterranean coast of

Chile corresponds to a climatic and vegetational transition zone and is considered as an area sensitive to environmental changes due to anthropogenic impacts and climate alternations [6,9–12]. Indeed, historical records have emphasised the influence of anthropogenic activities on lakes in the region over the last 500 years [13,14]. In particular, intensive periods of land use, clear-cutting of native forest and the replacement by exotic plantation forestry (*Pinus radiata* and *Eucalyptus* spp.), wheat growing, urbanisation and industrialisation processes have caused changes in the trophic status, chemical composition and water quality of the lakes [13–16].

Regional studies in the Chilean Mediterranean Zone revealed that prehispanic native cultures had no significant impact on land use [17]. However, since the mid-sixteenth century, Spanish colonisation induced disturbances on the natural landscape. The introduction of the Mediterranean Hispanic Model of agriculture-livestock resulted in pronounced land-use changes [18,19]. In addition, the urbanisation of the coastal zone has intensified over the last decades and generated a significant increase in nutrient inputs to watersheds, leading to gradual environmental degradation and an increase in phytoplankton productivity [13,16,20–23]. For example, diatom studies in Laguna Grande and Laguna Chica (San Pedro de la Paz, Biobío region, south-central Chile) revealed that trophic state changes occurred after the Spanish arrival [13,20,22]. Moreover, cyanobacterial blooms have been detected in Laguna Grande in the last decades [24], which is likely related to the recent increase in temperature due to global warming and increased nutrient concentrations [25–27].

However, few studies focused on long-term changes in the entire phytoplankton community have been considered in Chilean coastal lakes to explain their response to environmental conditions [6,9,28–30]. Sedimentological and biological proxies such as (sub)fossil remains, total organic carbon concentration, C and N stable isotopes and phytoplankton pigments can provide valuable information on past changes in primary production and the phytoplankton community structure [6,7,31–39]. Phytoplankton pigments have the advantages that they also allow for the study of soft-bodied organisms which do not readily fossilise. A disadvantage is that pigments are relatively sensitive to degradation in response to high irradiance, oxygen concentrations, bacterial activity, grazing and high temperatures [34,36,40–44]. Nevertheless, once buried in suitable conditions (anoxic sediments), pigments can be preserved for thousands of years [42,45–47]. Stable isotope ratios of carbon and nitrogen and the atomic C/N ratios can provide insights into the origin of organic matter in aquatic ecosystems, vegetation sources, aquatic algae proportions or terrestrial organic matter. Moreover, they are used to interpret paleoenvironmental changes in lakes and their watersheds [4,48–51]. The tracking of environmental changes allows historical trajectories, local and regional patterns to be revealed [11,52,53].

This paper is aimed at reconstructing primary production during the late Holocene to the present-day based on a multiproxy approach, which includes the sedimentological description, biogenic silica, carbon and nitrogen isotopic composition and fossil pigments in two Mediterranean coastal lakes in Chile, namely Laguna Grande and Chica de San Pedro. We focussed on the late Holocene because this period is characterised by profound land-use changes in the region [9,10,19,23].

2. Material and Methods

2.1. Study Area

The study area is located within the lacustrine system of San Pedro de la Paz, Biobío region, in south-central Chile [13,15]. The lacustrine system comprises two lakes; i.e., Laguna Grande (36°51' S; 73°06' O; 4 m.a.s.l.) and Laguna Chica (36°51' S; 73°05' O; 5 m.a.s.l.), referred to as LGSP and LCSP, respectively. Both lakes are part of an ancient coastal plain formed during the Quaternary [54,55]. The formation of the lakes is still largely unknown, but Martínez et al. [56] reported that both lakes were developed within the valley of ancient rivers that once drained into the Pacific Ocean. Subsequently, they were dammed due to the sedimentation contribution by the cliffs of the Nahuelbuta mountain range during the late Pleistocene/early Holocene. Additionally, basaltic sands transported from

the headwater to the mouth of the Biobío river originated by the Antuco Volcano (Lake Laja) contributed to the Biobío river delta formation and the Coronel coastal plain. These fluvial sediments were deposited at the north of the lakes as part of their geomorphological formation [56–58].

The lakes are located on the northwestern slope of the mountain range of Nahuelbuta, close to the Pacific Ocean and south of the Biobío River mouth [58] (Figure 1). The LGSP is a shallow lake with a 12.5 km² drainage basin, 1.55 km² surface area and 13.5 m maximum depth. Similarly, the LCSP is a small lake with a 4.5 km² drainage basin, 0.87 km² surface area and a maximum depth of 18 m (Table 1) [13,18,58]. Both systems show sharp slopes at the west, south and east sides, and soft slopes towards the north coast [13,56]. To date, the phytoplankton communities are dominated by Bacillariophyceae, Chlorophyceae, Desmidiaceae and Cyanobacteria (Table 1).

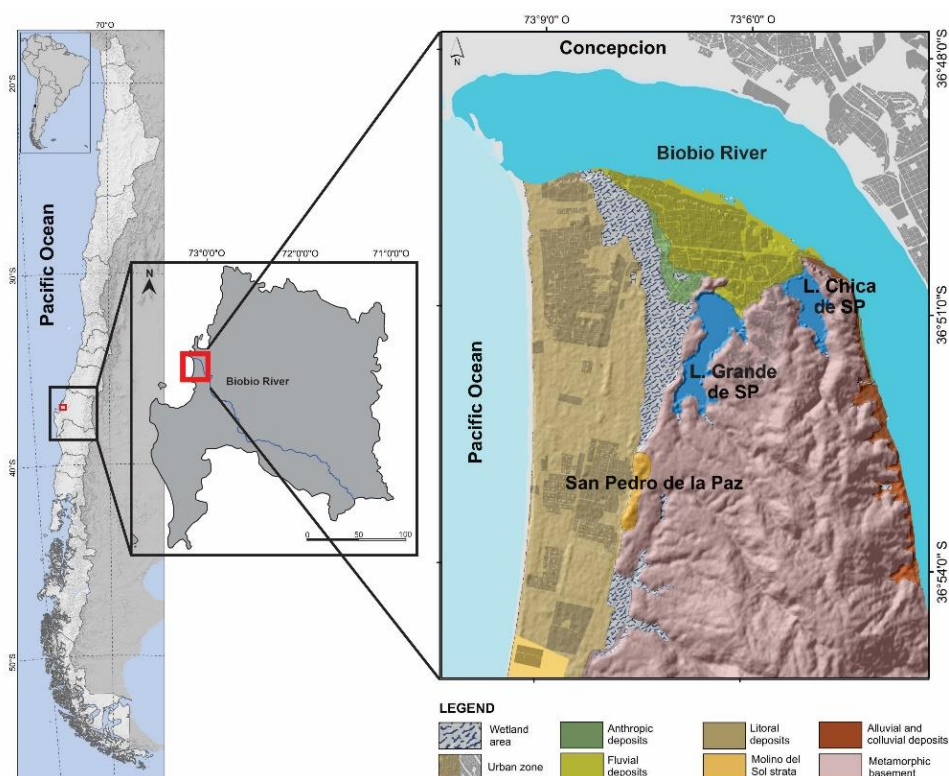


Figure 1. Study area of the Laguna Grande and Laguna Chica de San Pedro.

Table 1. Summary of environmental, physico-chemical and biological characteristics of the Laguna Grande and Laguna Chica de San Pedro (Parra 1989; Aranedo et al., 1999; Cisternas et al., 2000; Barra et al., 2001; Parra et al., 2003; Campos et al., 2005; Almanza et al., 2016).

	Laguna Chica	Laguna Grande
Latitude	36°51'	36°51'
Longitude	73°05'	73°06'
Altitude (m.a.s.l.)	5	4
Lake area (km ²)	0.82	1.55
Watershed area (km ²)	4.5	12.7
Maximum depth (m)	18	13.5
Volume (m ³ × 10 ⁶)	8.64	12.9
Native forest and shreds	27.1%	5.7%
Forest plantations	48.9%	52.4%
Agriculture	3.4%	1.0%

Table 1. Cont.

	Laguna Chica	Laguna Grande
Urban area	4.9%	4.1%
Water transparency (m)	5.2 (3.8–6.8)	3.7 (3.0–6.1)
Water temperature °C (min-max)	17.4 (12.5–24.0)	18.1 (12.2–24.0)
Annual mean precipitation (mm)	1.235 mm	1.235 mm
pH	7.0 (6.5–7.73)	7.0 (6.5–7.6)
Conductivity (µS/cm)	71 (50–90)	84 (35–107)
Dissolved oxygen (mg/L)	9.2 (5.9–10.9)	8.8 (4.9–10.7)
Alkalinity (meq/L CaCO ₃)	0.4 (0.4–0.5)	0.5 (0.5–0.6)
TDS (mg/L)	42.3	52.6
Total phosphorus TP (µg/L)	20	50
Total nitrogen TN (µg/L)	170 (60–320)	230 (80–340)
Chlorophyll <i>a</i> (µg/L)	1.20	6.42
Primary productivity (mgC/m ³ /hr)	2.44	22.68
Trophic state	Mesotrophic-Eutrophic	Eutrophic-Hypereutrophic
Macrophytes	Abundant	Major abundance
Summer stratification	Yes	No
Phytoplankton richness	39	57
Main phytoplankton groups	Bacillariophyceae Chlorophyceae Desmideaceae Cyanobacteria	Chlorophyceae Bacillariophyceae Desmideaceae Cyanobacteria
Reports of Cyanobacteria	<i>Microcystis</i> sp. (blooms) <i>Dolichospermum</i> sp. <i>Merismopedia</i> sp. <i>Oscillatoria</i> sp. <i>Aphanocapsa</i> sp.	<i>Microcystis</i> sp. (blooms) <i>Dolichospermum</i> sp. <i>Pseudoanabaena</i> sp. <i>Gomphosphaeria</i> sp. <i>Chroococcus</i> sp. <i>Snowella</i> sp.

Mean (min-max).

2.2. Sampling and Sedimentological Analysis

Duplicate sediment cores were collected in January 2016 at the central and the deepest part of LGSP (13.5 m) and LCSP (18 m). The cores were obtained using a UWITEC gravity corer equipped with a 6 cm diameter plexiglass tube, covered with aluminium foil to protect from sunlight and stored at 4 °C until the analyses. The cores were upward sectioned every 1 cm, freeze-dried and homogenised using a mortar and pestle to analyse biogenic silica and fossil pigments. For determination of the stable isotopes, the samples were oven-dried and homogenised using a mortar and pestle before the analysis. The biogenic silica (BSi) was extracted with the alkaline method and determined by molybdate-blue spectrophotometry [59].

The magnetic susceptibility (MS) was measured at 1 cm intervals using the Bartington MS2E sensor and the Multisus v2.44 software. The grain-size analysis was performed using a Malvern Mastersizer 3000 laser particle size analyser. A quantity of 5 mg of each sediment layer was treated with H₂O₂ (30%) in a thermal bath to remove the organic matter and then combined with distilled water to suspend sediments uniformly prior to analysis. The percentage by volume of each size fraction was analysed using the Gradistat program to determine conventional particle size statistics [60,61]. Grain-size and magnetic susceptibility were used as an indicator of input of terrigenous materials, allochthonous to the lake. These analyses were conducted in the laboratory of Paleolimnology and the laboratory of Environmental Sciences Center EULA-Chile at the University of Concepción, Chile.

2.3. Sediment Core Dating

The chronology of the sediment cores of LGSP and LCSP was established by combining ^{210}Pb , ^{137}Cs and ^{14}C . Short-lived radioisotope activities were measured by spectrometry using a low-background well-shaped high-efficiency, germanium spectrometer equipped with a Cryo-Cycle in the laboratory Environnements et Paléoenvironnements Océaniques et Continentaux (EPOC), Université de Bordeaux, France. Excess ^{210}Pb ($^{210}\text{Pb}_{\text{xs}}$) was calculated by subtracting the activity supported by its parent isotope, ^{226}Ra , from the total ^{210}Pb activity in the sediment. The activities of $^{210}\text{Pb}_x$ in excess ($^{210}\text{Pb}_{\text{xs}}$) and ^{137}Cs were analysed downcore until negligible values were observed, which was at about 20 and 14 cm for LGSP and LCSP, respectively. The AMS radiocarbon analyses (^{14}C) were performed on the bulk sediment samples, selecting three samples for LGSP and LCSP. These values were calibrated with Oxcal 3.10 [62] using the calibration curve SHCal 13 [63]. Mass accumulation rates (MAR, expressed in $\text{g m}^{-2} \text{cm}^{-1}$) were obtained by plotting the regression of $^{210}\text{Pb}_{\text{xs}}$ against cumulative mass and were used to calculate sediment ages. This approach assumes that the sediment surface represents the year of core acquisition. The artificial radioisotope ^{137}Cs was used as an independent time marker in order to validate the ^{210}Pb age model. All the ^{14}C and $^{210}\text{Pb}_{\text{xs}}$ dates were logged to the Clam code [64] using the R software [65] to obtain the chronological model. A cubic spline and linear interpolation allowed the ages of undated levels to be estimated.

2.4. Stable Isotopes

The analyses of stable isotopes of carbon and nitrogen were performed using an IsoPrime100, isotopic ratio mass spectrometry (Isoprime, UK) coupled in a continuous flow to a Vario Micro cube elemental analyser (Elementar, Germany) at the Laboratory of Oceanology, Institute of Chemistry, Université de Liege, Belgium. The isotopic values are expressed as δ values in ‰. Accuracy was obtained on 7 and 10 replicates for LGSP and LCSP, respectively, performed on samples and standards, i.e., standard atropine value (0.5 ‰ C and 0.4 ‰ N), IAEA-CH6 sucrose ($\delta^{13}\text{C} = -10.4 \pm 0.2\text{‰}$) and IAEA-N1 ($\delta^{15}\text{N} = +0.4 \pm 0.2\text{‰}$). The samples were acidified with HCl to remove inorganic carbonates to avoid any modification of nitrogen isotopic signature [18,66–68]. The total organic carbon (TOC) and carbon and nitrogen isotopes were used to discriminate between the allochthonous input and the autochthonous organic matter related to the productivity of the lake.

2.5. Pigment Analysis

Thirty samples of freeze-dried sediments were extracted from sediments in the cores of both lakes. A solution of 90% acetone was added to the samples, and sonication was used for the extraction (1 min per sample and let the extract rest overnight at 4 °C in dark conditions). The analyses were performed using the Agilent 1100 HPLC (high-performance liquid chromatography), pump, auto-sampler, DAD-diode-array detector and Agilent Eclipse XDB-C8 column [69]. The pigments were identified and quantified based on the retention time and specified spectrum of each pigment. They were calibrated using standard pigments provided by DHI Denmark.

The individual pigment concentrations were calculated using the response factors of standard pigments, expressed as dry-mass specific concentrations (μg pigment per mg dry sediment) [32,36,70,71]. The fossil pigments were assigned to their respective taxonomic groups. Chlorophylls, mainly represented by chlorophyll-*a* (chl-*a*), were used as an indicator of total photosynthetic algal concentration and higher plants. Chlorophyll-*b* (chl-*b*) reflects the presence of green algae and higher plants [71]. The carotenoids zeaxanthin, canthaxanthin and echinenone, were used as indicators of cyanobacterial abundance (Cyanophyta). Lutein was used as a signature of green algae, euglenophytes and higher plants [33]. Alloxanthin is a measure of cryptophytes, and diatoxanthin occurs in diatoms, dinoflagellates and chrysophytes. Chlorophyll degradation products were mainly repre-

sented by phaeophytin-*a* and phaeophorbide-*a* [37,69–72]. These analyses were performed in the Laboratory of Protistology and Aquatic Ecology, Ghent University, Belgium.

The total chlorophyll was estimated by calculating the sum of the chl-*a* and their degradation products (Phaeophorbide and Phaeophytin). Each pigment was divided by total chlorophyll to obtain pigment proportions. The carotenoid pigments were calculated considering the total carotenoids as the sum of zeaxanthine, canthaxanthin, echinenone, lutein, alloxanthin and diatoxanthin [31,72,73]. Pigment fluxes were treated as proxies of phytoplankton abundance using the sedimentation rate [72,73].

3. Results

3.1. Age Model

Radiocarbon ages from LGSP and LCSP cores are summarised in Table 2 and represented in Figure 2. The obtained ages maintain a stratigraphic order throughout the profile in both cores, covering the past 5000 years within 80 cm for LGSP and 2500 years within 116 cm for LCSP. The ^{14}C age model in LCSP is poorly resolved. Profiles of $^{210}\text{Pb}_{\text{xs}}$ show an exponential decrease of activities, from 40 mBq g $^{-1}$ for LGSP and 60 mBq g $^{-1}$ for LCSP in the uppermost sediments to negligible values in depth. The limit value of ^{210}Pb in excess to 1888 AD was observed at 25 cm for LGSP and 14 cm for LCSP. (Figures 2a and 2c). ^{137}Cs profiles in the two lakes present a peak at 12 cm (1965 \pm 5 AD) for LGSP and 5 cm (1965 \pm 8 AD) for LCSP, respectively (Figure 2b,d), which is in close agreement with the well-known pulse inputs related to the nuclear weapon test fallout in the early sixties (maximum atmospheric fallout is in 1965 in the Southern Hemisphere) [74].

Table 2. Radiocarbon date of bulk sediments from the Laguna Grande and Laguna Chica de San Pedro.

Lab Code	Lake	Core Depth (cm)	^{14}C yr BP $\pm 1\sigma$	Calibrate Age BC/AD		
				Min	Mean	Max
ETH-70456	Laguna grande	41	1707 \pm 23	339	385	431
ETH-70457	Laguna grande	51	2276 \pm 24	−325	−267	−209
ETH-70458	Laguna grande	71	3467 \pm 25	−1780	−1707	−1635
D-AMS 025916	Laguna Chica	54.5	936 \pm 26	1129	1172	1216
D-AMS 025914	Laguna Chica	116.5	2482 \pm 43	−599	−503	−407

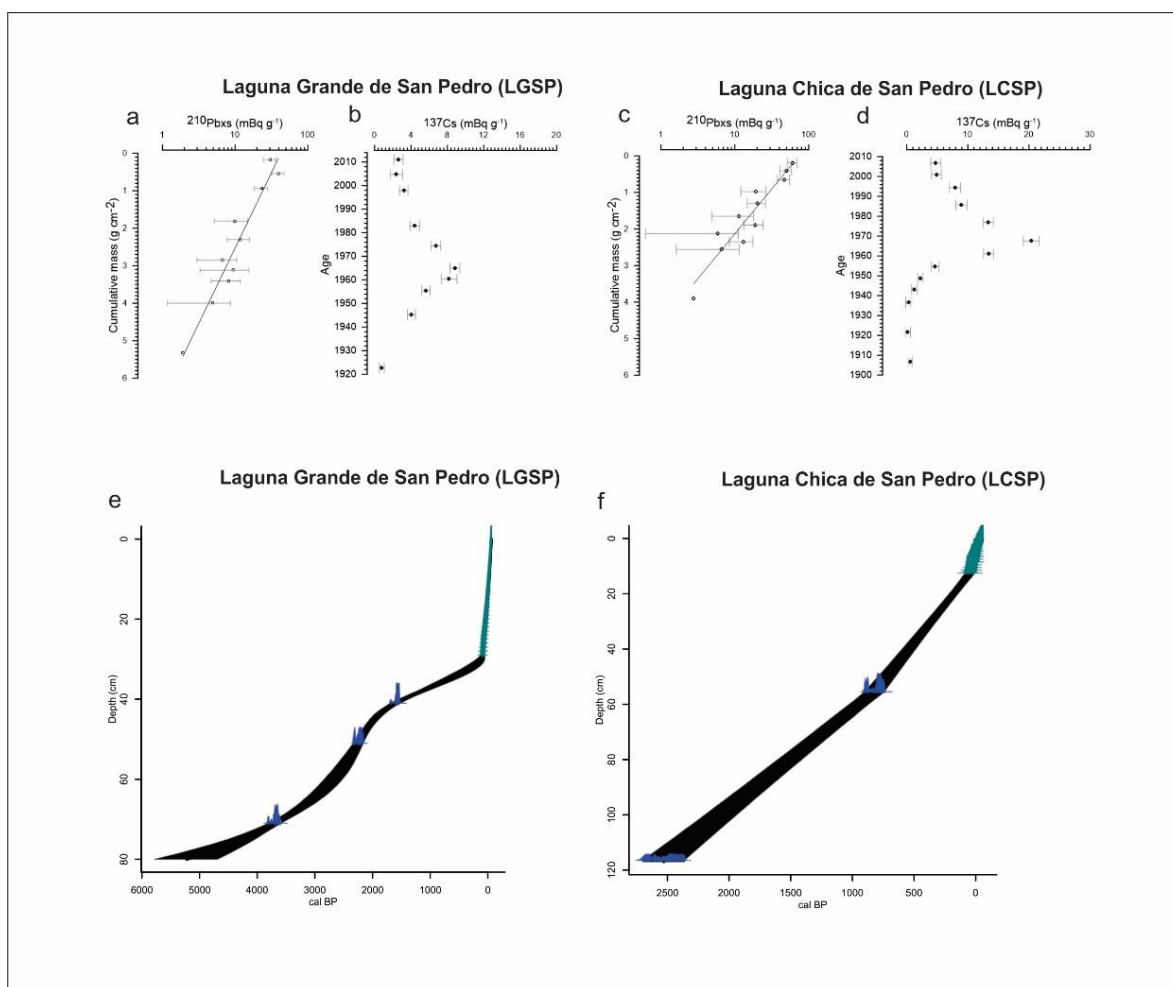


Figure 2. Chronology of the top centimetres of the Laguna Grande (a,b,e) and Laguna Chica (c,d,f) de San Pedro. The dark line represents the age model, while the grey shades represent the estimated errors, and the vertical and grey lines indicate the coring year.

3.2. Lithological Description

The sediment cores from LGSP and LCSP are characterised by two main units (Figure 3). The lower section is characterised by a light grey to beige coarser layer with higher MS values in both cores, whereas silty clay sediments compose the upper finer section.

Laguna Grande de San Pedro (LGSP)

The basal unit (58–47 cm) is mainly composed of silty sand. The sand fraction $> 63 \mu\text{m}$ averaged $14.5 \pm 3.8\%$ (Table 3). The highest MS values compared to the rest of the sediment core, averaged $299 \pm 149.9 \times 10^{-8}$. TOC and TN displayed a gradual increase from the bottom upwards, from 0.5 to 1.7‰ and 0.05 to 0.17‰, respectively. BSi concentrations were low, ranging from 0.35 to 1.19% ($0.79 \pm 0.24\%$). The C/N ratio varied from 8.7 to 10.3 (9.4 ± 0.5). The $\delta^{13}\text{C}$ was stable, ranging between -25.8% to -26.2% ($\pm 0.3\%$). Slight variations in $\delta^{15}\text{N}$ values ranged from 3.04 to 5.01‰ ($3.63 \pm 0.4\%$) at the bottom with a maximum at 48 cm.

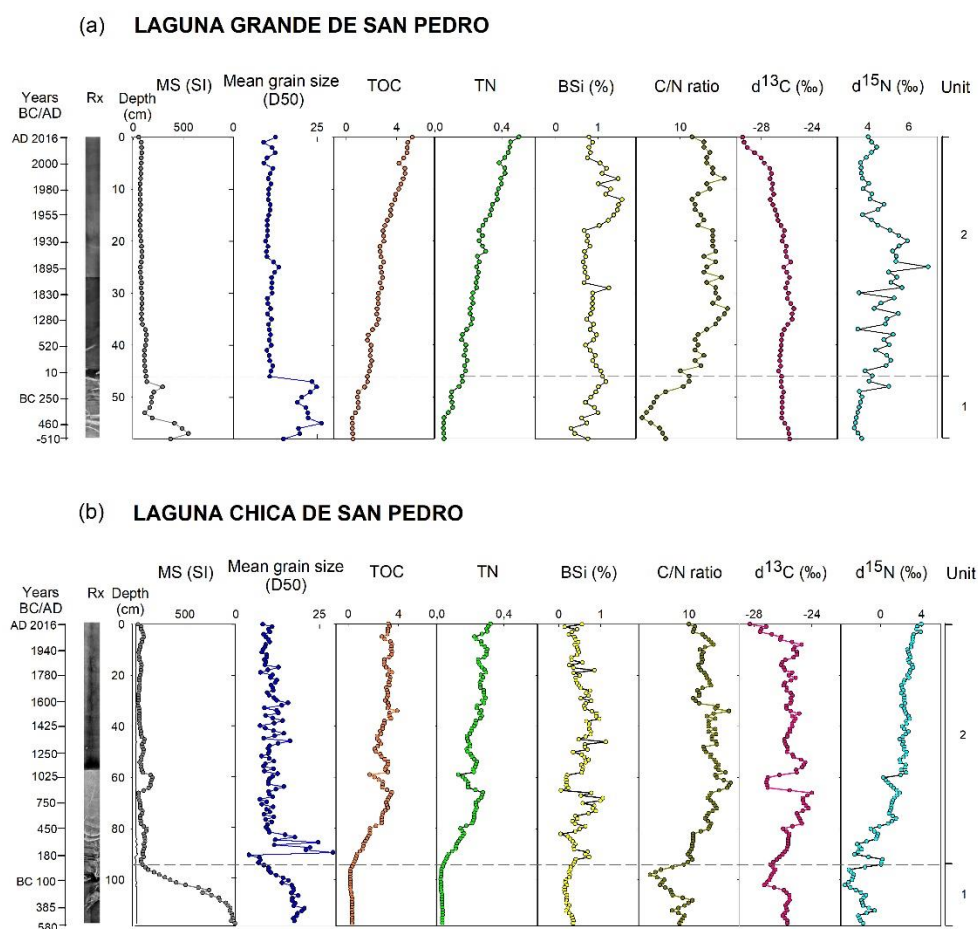


Figure 3. Depth profiles of magnetic susceptibility (SI), organic matter (%), biogenic silica (%), TOC (weight %), C/N ratio atomic, $\delta^{13}\text{C}$ (‰) and $\delta^{15}\text{N}$ (‰) in sediment core of (a) Laguna Grande de San Pedro (LGSP) and (b) Laguna Chica de San Pedro (LCSP).

Table 3. Composition of the sediment grain-size (mean percentage \pm standard deviation) of the Laguna Grande (LGSP) and Laguna Chica de San Pedro (LCSP) described by lithological units.

Laguna Grande de San Pedro			
	Clay (%)	Silt (%)	Sand (%)
UNIT 2 (46–0 cm)	7.12 \pm 0.83	90.75 \pm 1.95	2.03 \pm 2.38
UNIT 1 (60–47 cm)	4.64 \pm 0.91	80.88 \pm 4.13	14.48 \pm 3.76
Laguna Chica de San Pedro			
	Clay (%)	Silt (%)	Sand (%)
UNIT 2 (93–0 cm)	7.05 \pm 2.45	90.12 \pm 4.09	2.83 \pm 2.72
UNIT 1 (120–94cm)	4.68 \pm 1.62	87.82 \pm 2.86	7.50 \pm 2.65

Unit 2 (46–0 cm): the grain-size distribution was relatively stable, with a slight variation at the top of the core, with a high amount of silt fraction (~91%). Steady low MS values ($85.6 \pm 19.4 \times 10^{-8}$) were observed. Instead, TOC and TN profiles showed a gradual increase upward of this unit. BSi concentrations showed distinguished increases at 29, 12 and 8 cm, while values more than ten in C/N ratios were found from 46 cm to the top of the core. $\delta^{13}\text{C}$ values were stable from 46 to 6 cm, with a trend toward more negative values from 7 cm to the top. $\delta^{15}\text{N}$ values showed marked variations, extending from 3.5 to 6.9‰ ($4.6 \pm 0.7\text{‰}$), with a significant increase at 24 cm.

Laguna Chica de San Pedro (LCSP)

Unit 1 (117–94 cm): for LCSP (Figure 3b) showed the highest mean values at the bottom of the core for the mean grain size distribution ($15.3 \pm 3.8\%$) and the MS profile ($642 \pm 329 \times 10^{-8}$). In contrast, the lowest values were observed for TOC and TN (0.25 ± 0.07 and 0.03 ± 0.005 , respectively). BSi displayed relatively constant values, with an average of $0.5 \pm 0.23\%$. The C/N ratio fluctuated from 5.4 to 10.4, while the $\delta^{13}\text{C}$ and $\delta^{15}\text{N}$ showed more negative values at 102 cm.

Unit 2 (94–0 cm): the grain-size particle displayed variations throughout the core. Steady MS values were observed ($85.6 \pm 19.4 \times 10^{-8}$). A notable shift was observed in mean grain size, MS, TOC, TN, BSi, C/N, $\delta^{13}\text{C}$ and $\delta^{15}\text{N}$ between 66 and 58 cm.

3.3. Fossil Pigments Analysis

A total of ten fossil pigments were identified from the sediment core for LGSP (Figure 4a) and nine for LCSP (Figure 4b). Pigments concentrations were minimal in the sediment core’s deepest part and increased toward the upper layers, mainly in the modern sediments. A relatively high abundance of chlorophyll-*a* and phaeophytin-*a* for LGSP were observed. The abundance of canthaxanthin, echinenone and alloxanthin remained relatively low over time. Notable values were measured at 54, 36 and 9 cm for zeaxanthin and diatoxanthin, while lutein showed an increase between 9 and 4 cm. Chlorophyll-*b* was identified from 24 cm onwards, and phaeophorbide-*a* showed an increased trend upwards of the core from 24 cm. The total flux of chlorophylls and carotenoids remained low from the bottom, but relatively high flux was found at the end of the core (Figure 4b).

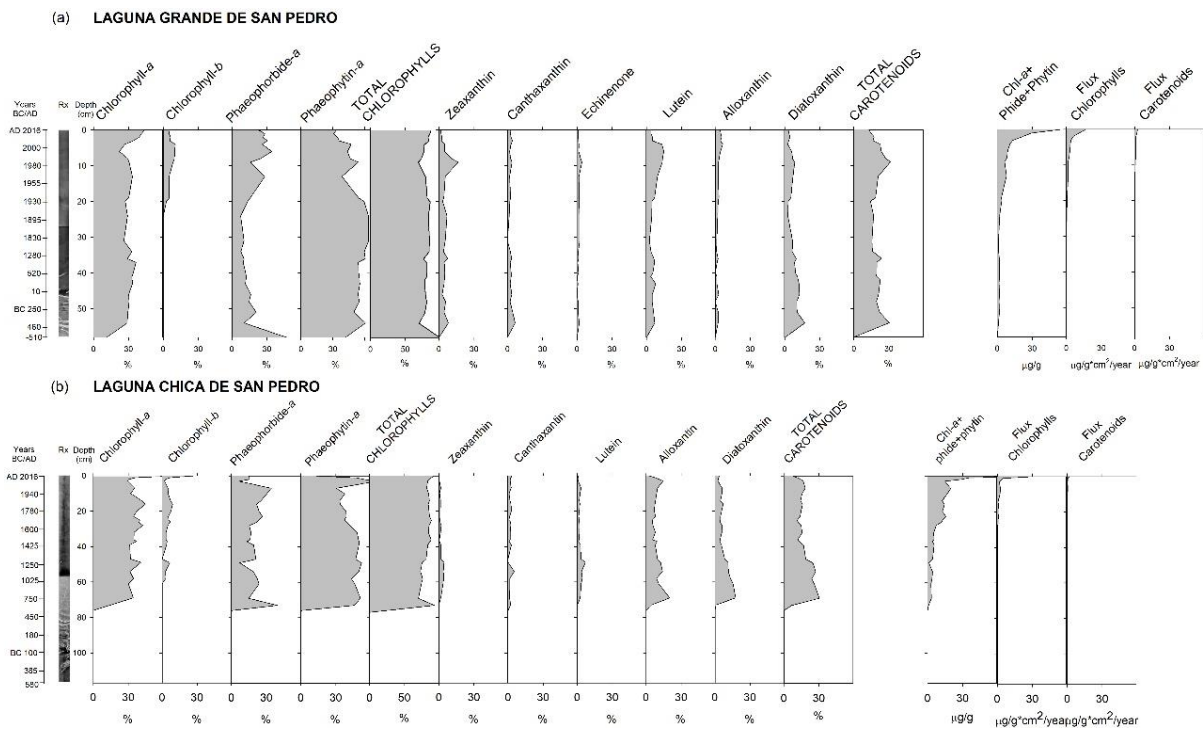


Figure 4. Fossil pigments stratigraphy of Laguna Grande (a) and Laguna Chica (b) de San Pedro sediment cores.

LCSP is characterised by a dominance of chl-*a*, phaeophytin-*a* and phaeophorbide-*a*. The chl-*b* was detected at 61 cm. Zeaxanthin, canthaxanthin and lutein displayed a relatively low abundance. Alloxanthin and diatoxanthin decreased gradually from 69 cm to the top of the core. The chlorophylls and carotenoid fluxes were relatively low at the bottom and increased in the upper sediments.

4. Discussion

4.1. Changes in Sediment Deposition

The changes in physical properties (mean grain size and magnetic susceptibility), as well as ^{137}Cs and the ^{210}Pb excess activities, were used to correlate both cores, since they did not present the same sedimentation rates with differences in the time window for both lakes (Figure 5). Although LGSP and LCSP have steep slopes on the south, east and west banks, the northern coast shows mild degradations [21,23]. The watershed area and the characteristics of the slopes of LCSP could have facilitated the dragging of particles with a more significant accumulation process on the bottom and; therefore, a higher sedimentation rate than in Laguna Grande, evidencing this change at 48 cm for LGSP and 98 cm for LCSP.

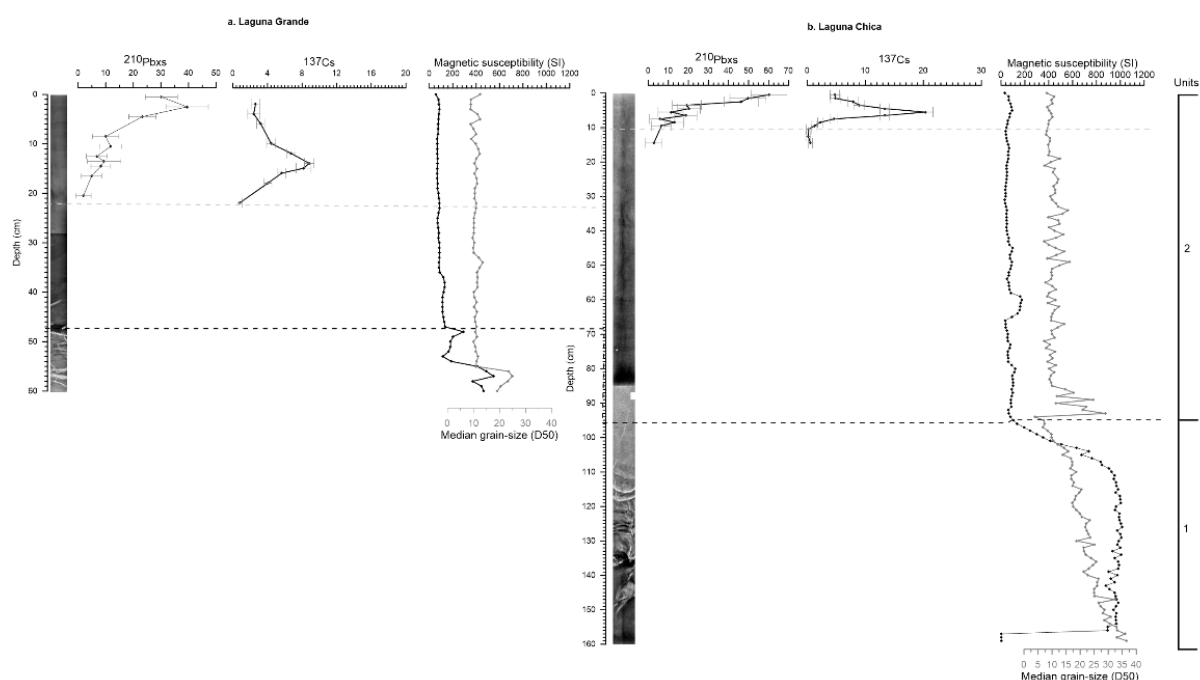


Figure 5. Correlation of ^{210}Pb , ^{137}Cs , magnetic susceptibility and grain size profiles of the Laguna Grande (a) and Laguna Chica (b) de San Pedro.

The main sedimentological change (i.e., coarse grain size, high MS) observed at the base of both studied cores most likely related to change in the sediment supply at the local scale. According to the reconstructed age models, this change occurred within a similar time window, i.e., 100 BC–AD 150 in both cores. The presence of sandy sedimentation and the high magnetic susceptibility values could be attributed to significant changes in the terrigenous sediment inputs to the lakes. A higher variability of continental weathering conditions and sediment input have been documented in geomorphological and pedological studies, which may indicate a more changeable climate in the late Holocene after 3000 yr B.P., marked by the fluctuations in the influence of the westerlies [75]. Besides, C/N ratio and $\delta^{15}\text{N}$ values indicated contributions of autochthonous organic matter in both lakes [48–51].

Under those considerations, we interpreted it as a transition from an arid condition in the mid-Holocene to more humid late Holocene conditions (humidity and temperature) that could have favoured the establishment of a native arboreal forest in the watersheds approximately at 100 BC–AD 150 [8–10]. Precipitations driven by the westerly winds in the region could influence the erosion rate in the watersheds displayed at the bottom of the lakes [9]. Other events that occurred in the area were dismissed, such as sediment supplies from the Biobío river, marine transgressions, emerged marine terraces and surface uplift rates, because they did not coincide with our period identified [56–58,76].

4.2. Late Holocene Evolution of Lake Primary Production

A gradual increase in the TOC and TN for LGSP and LCSP was reflected at 100 BC–AD 150 onwards and reached a maximum during the present-day period (Figure 3a,b). This trend might suggest increased diagenetic processes that, with time, led to the gradual breakdown of organic matter [2,65]. Nevertheless, this gradual increasing trend is absent in the LCSP record, which is, by contrast, characterised by relatively lower values of TOC and TN, but also BSi and $\delta^{13}\text{C}$, between 850 and 1050 AD, pointing out very low lake paleoproductivity. These results might suggest moist and cold conditions coinciding with persistent cool La Niña-like conditions between 650 and 950 AD, as reported by Fletcher and Moreno in Laguna San Pedro (38 °S) [11].

Variations of the C/N ratio and $\delta^{15}\text{N}$ were observed from 100 BC–AD 150 to the present day and particularly, from 450 AD and 520 AD in LCSP and LGSP, respectively. This might be related to an increased organic matter input derived from the watershed area of the lakes, but probably also increased the lake primary production as evidenced by the fossil pigment data. Indeed, fossil pigments were detected in LCSP from 450 AD onwards and were not present prior to this period. The carotenoids identified suggest the presence of cyanobacteria, chlorophyta, bacillariophyta and dinoflagellates (Figure 4a) in LCSP. In the LGSP, pigments were detected throughout the entire core, albeit at low concentrations prior to 1900 AD. Jenny et al. in Laguna Aculeo (34 °S) [9], reported that around 500–700 AD was characterised by a high frequency of flooding, an event that could have influenced the watersheds, dragging allochthonous matter towards the lakes, leading to changes in C/N, $\delta^{15}\text{N}$, TOC, TN and primary production during this period.

Interestingly, no obvious changes were present in the proxy records coincident and immediately after the Spanish colonisation in the region, around the middle of the XVI century (1536 to 1541 AD). Nevertheless, the highest values of C/N, which indicated a mixture of terrestrial and aquatic organic matter around 1550 AD for both lakes, resulting in higher catchment erosion and an increasing lake terrigenous supply, could be due to the settlements in the watershed. According to historical records described by Aronson et al. [77] and Torrejon and Cisternas [18], the Mapuches lacked intensive productive activities before the Spanish settlements. Accordingly, little impact was generated in these watersheds. Contrarily, in the middle of the XVI century, the Spanish colonisation at the south of the Biobío river caused the introduction of intensive exotic crops and livestock of ungulates (horses, sheep and cattle) [14,17,21,23,24,77,78]. It has been previously suggested that the development of settlements had a moderate impact on the pre-Columbian ecological landscape [19,78], which could favour the inputs of organic matter to the aquatic systems observed in C/N values as a possible signal of those changes.

The most obvious changes in the proxy records occurred in recent decades in both sediment cores. In particular, the C/N ratio and $\delta^{13}\text{C}$ decreased in both lakes, while the total chlorophyll and carotenoid concentrations increased. Combined, this suggests that phytoplankton primary production increased in recent decades. Nevertheless, apart from an increase in Chl-*b*, no obvious changes were observed in the relative abundance of the other marker pigments, apart from a slight decrease in diatoxanthin.

Interestingly, this is more or less coincident with a decrease in BSi, which might suggest that diatoms and/or chrysophytes became less abundant, while chlorophytes became more dominant (higher Chl-*b*) in recent decades. However, it must be noted that the sharp rise in total pigments in the most recent samples might reflect diagenesis and the degradation of pigments with time.

Nevertheless, given the coincident rise in pigment concentration and the change in the other proxies (i.e., C/N ratio and $\delta^{13}\text{C}$), we suggest that lake primary production increased in the most recent decades. This is consistent with a period of high sedimentation rates, as described by Urrutia et al. [22] and Cisternas et al. [79], in LCSP from 1951 to 1968 AD, which coincided with our results showing an increase in C/N ratio and $\delta^{13}\text{C}$ at 1955 AD. While Cruces et al. [13] described this period in LGSP from 1948 to 1972 AD, which coincided with a significant increase in hydrocarbons, fatty acids and organic matter,

observed by BSi, C/N and $\delta^{15}\text{N}$ in the same period in this lake. The dynamic changes observed for both LGSP and LCSP lakes could be linked to the increased urbanisation of the surrounding areas, and mainly the creation of the Villa of San Pedro in 1962 [20], and the increase in summer houses for touristic and recreational activities on the banks of LCSP and LGSP [23]. Finally, an integrated management program is required to generate a regional plan of conservation and the strengthening of institutional frameworks to enable governance and public participation in these systems [80].

5. Conclusions

A reconstruction of primary production based on multiproxy analyses in Laguna Grande and Laguna Chica de San Pedro provided essential information about changes in the last 2500 years. The major sedimentological transition observed at the lower part of the sedimentary columns was attributed to local influence with an important proximal input in both lakes. Additionally, the westerlies winds also contributed to the terrigenous sediment inputs at 100 BC–AD 150. Laguna Chica de San Pedro evidenced a low primary production between 850 and 1050 AD that coincided with the persistent cool La Niña-like conditions. Historical records highlighted the transformations in the ecological landscape of the area during the colonisation, which were notable around 1550 AD in terms of the C/N results. The fossil pigment concentrations and the stable isotopes suggest increased phytoplankton primary production in both lakes in recent decades. These are likely the result of local environmental conditions and human disturbances related to urbanisation, the cutting and replacing of native forest and commercial logging. Hence, an integrated management program for these watersheds is highly needed. We recommend further research focused on primary production, climate and anthropogenic drivers to understand long-term responses and patterns of aquatic ecosystems at the local and regional scale.

Author Contributions: Conceptualisation and methodology, I.-Y.M., A.B.-M., N.F., M.E.O., G.L., D.A., F.T., R.U.; software, I.-Y.M., M.E.O., S.S., G.D., P.P.; validation, S.S., E.V., R.U.; formal analysis, I.-Y.M., A.B.-M., N.F., M.E.O., E.V., R.U.; investigation, I.-Y.M., A.B.-M., F.T.; writing—original draft preparation, I.-Y.M., A.B.-M.; writing—review and editing, I.-Y.M., A.B.-M., N.F., M.E.O., E.V., G.L., F.T., D.A., R.U.; visualisation, I.-Y.M., A.B.-M., G.D., P.P.; supervision, N.F., E.V., R.U.; project administration, I.-Y.M.; funding acquisition, I.-Y.M., N.F. All authors contributed to the work. All authors have read and agreed to the published version of the manuscript.

Funding: This research was funded by the National Research and Development Agency (ANID, according to its initials in Spanish), the project ANID/FONDAP/15130015), the ERASMUS PLUS, and the Wallonie-Bruxelles International and the National Autonomous University of Honduras (UNAH, according to its initials in Spanish).

Institutional Review Board Statement: Not applicable.

Informed Consent Statement: Not applicable.

Data Availability Statement: The data presented in this study are available on request from the corresponding author.

Acknowledgments: We would like to thank the Directorate for Scientific, Humanistic and Technological Research (DICIHT, according to its initials in Spanish), from the National Autonomous University of Honduras for sponsoring the publication, the Environmental Sciences Centre EULA-Chile laboratory and Ilse Daveloose for the contribution to the fossil pigment analysis (University of Ghent, Belgium).

Conflicts of Interest: The authors declare no conflict of interest. The funders had no role in the design of the study; in the collection, analyses, or interpretation of data; in the writing of the manuscript, or in the decision to publish the results.

References

1. Hakanson, L.; Jansson, M. *Principles of Lake Sedimentology*; Springer: Berlin/Heidelberg, Germany, 1983; Volume 330. [[CrossRef](#)]

2. Bertrand, S.; Boës, X.; Castiaux, J.; Charlet, F.; Urrutia, R.; Espinoza, C.; Lepoint, G.; Charlier, B.; Fagel, N. Temporal evolution of sediment supply in Lago Puyehue (Southern Chile) during the last 600 yr and its climatic significance. *Quat. Res.* **2005**, *64*, 163–175. [[CrossRef](#)]
3. Schindler, D.W. Lakes as sentinels and integrators for the effects of climate change on watersheds, airsheds, and landscapes. *Limnol. Oceanogr.* **2009**, *54*, 2349–2358. [[CrossRef](#)]
4. Ahmad, K.; Davies, C. Stable isotope ($\delta^{13}\text{C}$ and $\delta^{15}\text{N}$) based interpretation of organic matter source and paleoenvironmental conditions in Al-Azraq basin, Jordan. *Appl. Geochem.* **2017**, *78*, 49–60. [[CrossRef](#)]
5. Maberly, S.C.; O'Donnell, R.A.; Woolway, R.I.; Cutler, M.E.J.; Gong, M.; Jones, I.D.; Merchant, C.J.; Miller, C.A.; Politi, E.; Scott, E.M.; et al. Global lake thermal regions shift under climate change. *Nat. Commun.* **2020**, *11*, 1232. [[CrossRef](#)] [[PubMed](#)]
6. Birks, H.J.B. Multi-proxy studies in palaeolimnology. *Veg. Hist. Archaeobot.* **2006**, *15*, 235–251. [[CrossRef](#)]
7. Leavitt, P.R.; Fritz, S.C.; Anderson, N.J.; Baker, P.A.; Blenckner, T.; Bunting, L.; Catalán, D.J.C.; Hobbs, W.O.; Jeppesen, E.; Korhola, A.; et al. Paleolimnological evidence of the effects on lakes of energy and mass transfer from climate and humans. *Limnol. Oceanogr.* **2009**, *54*, 2330–2348. [[CrossRef](#)]
8. Villa-Martínez, R.; Villagrán, C. Historia de la vegetación de bosques pantanosos de la costa de Chile central durante el Holoceno medio y tardío. *Rev. Chil. Hist. Nat.* **1997**, *70*, 391–401.
9. Jenny, B.; Valero-Garcés, B.L.; Villa-Martínez, R.; Urrutia, R.; Geyh, M.; Veit, H. Early to Mid-Holocene Aridity in Central Chile and the Southern Westerlies: The Laguna Aculeo Record (34°S). *Quat. Res.* **2002**, *58*, 160–170. [[CrossRef](#)]
10. Maldonado, A.; Villagrán, C. Climate variability over the last 9900 cal yr BP from a swamp forest pollen record along the semiarid coast of Chile. *Quat. Res.* **2006**, *66*, 246–258. [[CrossRef](#)]
11. Fletcher, M.-S.; Moreno, P.I. Vegetation, climate and fire regime changes in the Andean region of southern Chile (38°S) covaried with centennial-scale climate anomalies in the tropical Pacific over the last 1500 years. *Quat. Sci. Rev.* **2012**, *46*, 46–56. [[CrossRef](#)]
12. Frugone-Álvarez, M.; Latorre, C.; Giralt, S.; Polanco-Martínez, J.; Bernárdez, P.; Oliva-Urcia, B.; Maldonado, A.; Carvedo, M.L.; Moreno, A.; Huertas, A.D.; et al. A 7000-year high-resolution lake sediment record from coastal central Chile (Lago Vichuquén, 34°S): Implications for past sea level and environmental variability. *J. Quat. Sci.* **2017**, *32*, 830–844. [[CrossRef](#)]
13. Cruces, F.; Urrutia, R.; Araneda, A.; Torres, L.; Cisternas, M.; Vyverman, W. Evolución trófica de Laguna Grande de San Pedro (VIII Región, Chile) durante el último siglo, mediante el análisis de registros sedimentarios. *Rev. Chil. Hist. Nat.* **2001**, *74*, 407–418. [[CrossRef](#)]
14. Cisternas-Vega, M.; Torrejón-Godoy, F. Cambios de Uso del Suelo, Actividades Agropecuarias e Intervención Ambiental Temprana en una Localidad fronteriza de la Araucanía (S. XVI-XIX). *Rev. Geogr. Norte Gd.* **2002**, *29*, 83–94.
15. Chirinos, L.; Rose, N.; Urrutia, R.; Muñoz, P.; Torrejón, F.; Torres, L.; Cruces, F.; Araneda, A.; Zaror, C. Environmental evidence of fossil fuel pollution in Laguna Chica de San Pedro lake sediments (Central Chile). *Environ. Pollut.* **2006**, *141*, 247–256. [[CrossRef](#)] [[PubMed](#)]
16. Fuentealba, C.; Henríquez, O. Rol de las poblaciones de *Diplodon chilensis* (Gray, 1828) (Bivalvia: HYRIIDAE) en el estado trófico de la Laguna Chica de San Pedro (Chile). *Commun. Soc. Malacol. Urug.* **2009**, *9*, 195–200. Available online: <https://www.redalyc.org/articulo.oa?id=52414008003> (accessed on 14 September 2019).
17. Adán, L.; Rodrigo, M.; Navarro, X.; Campbell, R.; Quiroz, D.; Sánchez, M. Historia prehispánica de la región Centro-Sur de Chile: Cazadores-recolectores holocénicos y comunidades alfareras (ca. 10.000 años a.C. a 1.550 años d.C.). In *Prehistoria en Chile: Desde sus Primeros Habitantes Hasta Los Incas*; Falabella, F., Uribe, M., Sanhueza, L., Aldunate, C., Hidalgo, J., Eds.; Editorial Universitaria: Santiago, Chile, 2016; pp. 401–441.
18. Torrejón, F.; Cisternas, M. Alteraciones del paisaje ecológico araucano por la asimilación mapuche de la agroganadería hispano-mediterránea (siglos XVI y XVII). *Rev. Chil. Hist. Nat.* **2002**, *75*, 729–736. [[CrossRef](#)]
19. Torrejón, F.; Cisternas, M. Impacto ambiental temprano en la Araucanía deducido de crónicas españolas y estudios historiográficos. *Bosque* **2003**, *24*, 45–55. [[CrossRef](#)]
20. Parra, O. La eutroficación de la Laguna Grande de San Pedro, Concepción, Chile: Un caso de estudio. *Ambient. Desarro.* **1989**, *1*, 117–136.
21. Cisternas, M.; Torres, L.; Urrutia, R.; Araneda, A.; Parra, O. Comparación ambiental, mediante registros sedimentarios, entre las condiciones prehispánicas y actuales de un sistema lacustre. *Rev. Chil. Hist. Nat.* **2000**, *73*, 151–162. [[CrossRef](#)]
22. Urrutia, R.; Koen, S.; Cruces, F.; Pozo, K.; Becerra, J.; Araneda, A.; Vyverman, W.; Parra, O. Paleolimnological studies of Laguna Chica of San Pedro (VIII Region): Diatoms, hydrocarbons and fatty acid records. *Rev. Chil. Hist. Nat.* **2000**, *73*, 717–728. [[CrossRef](#)]
23. Parra, O.; Valdovinos, C.; Urrutia, R.; Cisternas, M.; Habit, E.; Mardones, M. Caracterización y tendencias tróficas de cinco lagos costeros de Chile Central. *Limnetica* **2003**, *22*, 51–83.
24. Almanza, V.; Parra, O.; Bicudo, C.E.D.M.; González, M.A.; Lopez, M.; Urrutia, R. Floraciones de fitoplancton y variación de la estructura comunitaria fitoplanctónica en tres lagos someros eutróficos de Chile Central. *Gayana Bot.* **2016**, *73*, 191–205. [[CrossRef](#)]
25. Wanner, H.; Beer, J.; Bütikofer, J.; Crowley, T.J.; Cubasch, U.; Flückiger, J.; Goosse, H.; Grosjean, M.; Joos, F.; Kaplan, J.O.; et al. Mid- to Late Holocene climate change: An overview. *Quat. Sci. Rev.* **2008**, *27*, 1791–1828. [[CrossRef](#)]
26. Paerl, H.W.; Paul, V.J. Climate change: Links to global expansion of harmful cyanobacteria. *Water Res.* **2012**, *46*, 1349–1363. [[CrossRef](#)] [[PubMed](#)]
27. Woolway, R.I.; Kraemer, B.M.; Lenters, J.D.; Merchant, C.J.; O'Reilly, C.M.; Sharma, S. Global lake responses to climate change. *Nat. Rev. Earth Environ.* **2020**, *1*, 388–403. [[CrossRef](#)]

28. Jenny, B.; Valero-Garcés, B.L.; Urrutia, R.; Kelts, K.; Veit, H.; Appleby, P.G.; Geyh, M. Moisture changes and fluctuations of the Westerlies in Mediterranean Central Chile during the last 2000 years: The Laguna Aculeo record (33°50'S). *Quat. Int.* **2002**, *87*, 3–18. [[CrossRef](#)]
29. Leavitt, P.R.; Cumming, B.F.; Smol, J.P.; Reasoner, M.; Pienitz, R.; Hodgson, D.A. Climatic control of ultraviolet radiation effects on lakes. *Limnol. Oceanogr.* **2003**, *48*, 2062–2069. [[CrossRef](#)]
30. Pal, S.; Gregory-Eaves, I.; Pick, F.R. Temporal trends in cyanobacteria revealed through DNA and pigment analyses of temperate lake sediment cores. *J. Paleolimnol.* **2015**, *54*, 87–101. [[CrossRef](#)]
31. Züllig, H. Untersuchungen über die Stratigraphie von Carotinoiden im geschichteten Sediment von 10 Schweizer Seen zur Erkundung früherer Phytoplankton-Entfaltungen. *Aquat. Sci.* **1982**, *44*, 1–98. [[CrossRef](#)]
32. Leavitt, P.R.; Hodgson, A. Sedimentary pigments. In *Tracking Environmental Change Using Lake Sediments: Terrestrial, Algal and Siliceous Indicators*; Smol, J.P., Birks, H.J.B., Last, W.M., Eds.; Kluwer Academic Publishers: New York, NY, USA, 2001; Volume 3, pp. 295–325. [[CrossRef](#)]
33. Lami, A.; Musazzi, S.; Marchetto, A.; Buchaca, T.; Kernan, M.; Jeppesen, E.; Guilizzoni, P. Sedimentary pigments in 308 alpine lakes and their relation to environmental gradients. *Adv. Limnol.* **2009**, *62*, 247–268. [[CrossRef](#)]
34. Bianchi, T.S.; Canuel, E.A. *Chemical Biomarkers in Aquatic Ecosystems*; Princeton University Press: Princeton, NJ, USA, 2011; Volume 392. [[CrossRef](#)]
35. Gregory-Eaves, I.; Beisner, B.E. Palaeolimnological insights for biodiversity science: An emerging field. *Freshw. Biol.* **2011**, *56*, 2653–2661. [[CrossRef](#)]
36. Schneider, T.; Rimer, D.; Butz, C.; Grosjean, M. A high-resolution pigment and productivity record from the varved Ponte Tresa basin (Lake Lugano, Switzerland) since 1919: Insight from an approach that combines hyperspectral imaging and high-performance liquid chromatography. *J. Paleolimnol.* **2018**, *60*, 381–398. [[CrossRef](#)]
37. Sanchini, A.; Grosjean, M. Quantification of chlorophyll a, chlorophyll b and pheopigments a in lake sediments through deconvolution of bulk UV–VIS absorption spectra. *J. Paleolimnol.* **2020**, *64*, 243–256. [[CrossRef](#)]
38. Sanchini, A.; Szidat, S.; Tylmann, W.; Vogel, H.; Wacnik, A.; Grosjean, M. A Holocene high-resolution record of aquatic productivity, seasonal anoxia and meromixis from varved sediments of Lake Łazduny, North-Eastern Poland: Insight from a novel multi-proxy approach. *J. Quat. Sci.* **2020**, *35*, 1070–1080. [[CrossRef](#)]
39. Sanger, J.E. Fossil pigments in paleoecology and paleolimnology. *Palaeogeogr. Palaeoclim. Palaeoecol.* **1988**, *62*, 343–359. [[CrossRef](#)]
40. Cuddington, K.; Leavitt, P.R. An individual-based model of pigment flux in lakes: Implications for organic biogeochemistry and paleoecology. *Can. J. Fish. Aquat. Sci.* **1999**, *56*, 1964–1977. [[CrossRef](#)]
41. Kowalewska, G. Algal pigments in Baltic sediments as markers of ecosystem and climate changes. *Clim. Res.* **2001**, *18*, 89–96. [[CrossRef](#)]
42. Reuss, N.; Leavitt, P.R.; Hall, R.I.; Bigler, C.; Hammarlund, D. Development and application of sedimentary pigments for assessing effects of climatic and environmental changes on subarctic lakes in northern Sweden. *J. Paleolimnol.* **2009**, *43*, 149–169. [[CrossRef](#)]
43. Amann, B.; Lobsiger, S.; Fischer, D.; Tylmann, W.; Bonk, A.; Filipiak, J.; Grosjean, M. Spring temperature variability and eutrophication history inferred from sedimentary pigments in the varved sediments of Lake Żabińskie, north-eastern Poland, AD 1907–2008. *Glob. Planet. Chang.* **2014**, *123*, 86–96. [[CrossRef](#)]
44. Tse, T.; Doig, L.; Leavitt, P.; Quiñones-Rivera, Z.; Codling, G.; Lucas, B.; Liber, K.; Giesy, J.; Wheeler, H.; Jones, P. Long-term spatial trends in sedimentary algal pigments in a narrow river-valley reservoir, Lake Diefenbaker, Canada. *J. Great Lakes Res.* **2015**, *41*, 56–66. [[CrossRef](#)]
45. Gu, B.; Schelske, C.L.; Brenner, M. Relationship between sediment and plankton isotope ratios ($\delta^{13}\text{C}$ and $\delta^{15}\text{N}$) and primary productivity in Florida lakes. *Can. J. Fish. Aquat. Sci.* **1996**, *53*, 875–883. [[CrossRef](#)]
46. Verleyen, E.; Hodgson, D.A.; Leavitt, P.R.; Sabbe, K.; Vyverman, W. Quantifying habitat-specific diatom production: A critical assessment using morphological and biogeochemical markers in Antarctic marine and lake sediments. *Limnol. Oceanogr.* **2004**, *49*, 1528–1539. [[CrossRef](#)]
47. Deshpande, B.N.; Tremblay, R.; Pienitz, R.; Vincent, W.F. Sedimentary pigments as indicators of cyanobacterial dynamics in a hypereutrophic lake. *J. Paleolimnol.* **2014**, *52*, 171–184. [[CrossRef](#)]
48. Talbot, M.R.; Johannessen, T. A high resolution palaeoclimatic record for the last 27,500 years in tropical West Africa from the carbon and nitrogen isotopic composition of lacustrine organic matter. *Earth Planet. Sci. Lett.* **1992**, *110*, 23–37. [[CrossRef](#)]
49. Hassan, K.M.; Swinehart, J.B.; Spalding, R.F. Evidence for Holocene environmental change from C/N ratios, and $\delta^{13}\text{C}$ and $\delta^{15}\text{N}$ values in Swan Lake sediments, western Sand Hills, Nebraska. *J. Paleolimnol.* **1997**, *18*, 121–130. [[CrossRef](#)]
50. Talbot, M.R.; Lærdal, T. The Late Pleistocene—Holocene palaeolimnology of Lake Victoria, East Africa, based upon elemental and isotopic analyses of sedimentary organic matter. *J. Paleolimnol.* **2000**, *23*, 141–164. [[CrossRef](#)]
51. Routh, J.; Choudhary, P.; Meyers, P.A.; Kumar, B. A sediment record of recent nutrient loading and trophic state change in Lake Norrviken, Sweden. *J. Paleolimnol.* **2008**, *42*, 325–341. [[CrossRef](#)]
52. Gell, P.; Bennion, H.; Battarbee, R. Paleolimnology and the restoration of aquatic systems. *PAGES Newsl.* **2009**, *17*, 119–120. [[CrossRef](#)]
53. Malone, T.C.; Newton, A. The Globalization of Cultural Eutrophication in the Coastal Ocean: Causes and Consequences. *Front. Mar. Sci.* **2020**, *7*, 670. [[CrossRef](#)]

54. Cisternas, M.; Araneda, A.; Retamal, O.; Urrutia, R. Sedimentos como indicadores de eventos erosivos en una pequeña cuenca lacustre de Chile Central. *Espac. Desarro.* **1997**, *9*, 103–116.
55. Fagel, N.; Bertrand, S.; Mattioli, N.; Gilson, D.; Chirinos, L.; Lepoint, G.; Urrutia, R. Geochemical evidence (C, N and Pb isotopes) of recent anthropogenic impact in south-central Chile from two environmentally distinct lake sediment records. *J. Quat. Sci.* **2010**, *25*, 1100–1112. [[CrossRef](#)]
56. Martínez, C.; Rojas, C.; Rojas, O.; Quezada, J.; Lopez, P.; Ruiz, V. Crecimiento urbano sobre geofomas costeras de la llanura de San Pedro, área Metropolitana de Concepción. In *En las Costas del Neoliberalismo: Naturaleza, Urbanización y Producción Inmobiliaria: Experiencias en Chile y Argentina*; Hidalgo, R., Santana, D., Voltaire, A., Arenas, F., Salazar, A., Valdebenito, C., Alvarez, L., Eds.; No. 23; Geolibros: Santiago, Chile, 2016; pp. 287–312.
57. Dobry, R.; Poblete, M. Densidades máximas y mínimas de las arenas Bio-Bio. *Rev. IDIEM* **1966**, *5*, 151–159. Available online: <https://revistaidiem.uchile.cl/index.php/RIDIEM/article/view/38465> (accessed on 20 November 2020).
58. Isla, F.I.; Flory, J.Q.; Martínez, C.; Fernández, A.; Jaque, E. The evolution of the Bío Bío delta and the coastal plains of the Arauco Gulf, Bío Bío Region: The Holocene sea-level curve of Chile. *J. Coast. Res.* **2012**, *28*, 102–111. [[CrossRef](#)]
59. Mortlock, R.A.; Froelich, P.N. A simple method for the rapid determination of biogenic opal in pelagic marine sediments. *Deep. Sea Res. Part A Oceanogr. Res. Pap.* **1989**, *36*, 1415–1426. [[CrossRef](#)]
60. Blott, S.J.; Pye, K. GRADISTAT: A grain size distribution and statistics package for the analysis of unconsolidated sediments. *Earth Surf. Process. Landf.* **2001**, *26*, 1237–1248. [[CrossRef](#)]
61. Castro, J.M.T.; Vergara, C.; Alvarez, D.; Diaz, G.; Fierro, P.; Araneda, A.; Torrejón, F.; Rondanelli, M.; Fagel, N.; Urrutia, R. A new multi-proxy record of environmental change over the last 1000 years on Chiloé Island: Lake Pastahué, south-central Chile (42°S). *Holocene* **2018**, *29*, 421–431. [[CrossRef](#)]
62. Ramsey, C.B. *OxCal Program Version 3.10*; Manual; Oxford Radiocarbon Accelerator Unit: Oxford, UK, 2005; Available online: <https://c14.arch.ox.ac.uk/oxcal3/oxcal.htm> (accessed on 10 October 2020).
63. Hogg, A.G.; Hua, Q.; Blackwell, P.G.; Niu, M.; Buck, C.E.; Guilderson, T.P.; Heaton, T.J.; Palmer, J.G.; Reimer, P.J.; Reimer, R.W.; et al. SHCal13 Southern Hemisphere Calibration, 0–50,000 Years cal BP. *Radiocarbon* **2013**, *55*, 1889–1903. [[CrossRef](#)]
64. Blaauw, M. Methods and code for ‘classical’ age-modelling of radiocarbon sequences. *Quat. Geochronol.* **2010**, *5*, 512–518. [[CrossRef](#)]
65. R Development Core Team. *R: A Language and Environment for Statistical Computing*; Version 2.6.2; R Foundation for Statistical Computing: Vienna, Austria, 2016; Available online: <https://www.r-project.org/> (accessed on 14 September 2018).
66. Freudenthal, T.; Wagner, T.; Wenzhöfer, F.; Zabel, M.; Wefer, G. Early diagenesis of organic matter from sediments of the eastern subtropical Atlantic: Evidence from stable nitrogen and carbon isotopes. *Geochim. Cosmochim. Acta* **2001**, *65*, 1795–1808. [[CrossRef](#)]
67. Nysse, F.; Brey, T.; Lepoint, G.; Bouqueneau, J.-M.; De Broyer, C.; Dauby, P. A stable isotope approach to the eastern Weddell Sea trophic web: Focus on benthic amphipods. *Polar Biol.* **2002**, *25*, 280–287. [[CrossRef](#)]
68. Vaslet, A.; Bouchon-Navarro, Y.; Harmelin-Vivien, M.; Lepoint, G.; Louis, M.; Bouchon, C. Foraging habits of reef fishes associated with mangroves and seagrass beds in a Caribbean lagoon: A stable isotope approach. *Cienc. Mar.* **2015**, *41*, 217–232. [[CrossRef](#)]
69. Van Heukelem, L.; Thomas, C.S. Computer-assisted high-performance liquid chromatography method development with applications to the isolation and analysis of phytoplankton pigments. *J. Chromatogr. A* **2001**, *910*, 31–49. [[CrossRef](#)]
70. Meyer, I.; Van Daele, M.; Fiers, G.; Verleyen, E.; De Batist, M.; Verschuren, D. Sediment reflectance spectroscopy as a paleo-hydrological proxy in East Africa. *Limnol. Oceanogr. Methods* **2017**, *16*, 92–105. [[CrossRef](#)]
71. Reuss, N. Sediment Pigments as Biomarkers of Environmental Change. Ph.D. Thesis, University of Copenhagen, København, Denmark, 2005.
72. Verleyen, E.; Hodgson, D.A.; Sabbe, K.; Vyverman, W. Late Holocene changes in ultraviolet radiation penetration recorded in an East Antarctic lake. *J. Paleolimnol.* **2005**, *34*, 191–202. [[CrossRef](#)]
73. Legendre, P.; Gallagher, E.D. Ecologically meaningful transformations for ordination of species data. *Oecologia* **2001**, *129*, 271–280. [[CrossRef](#)] [[PubMed](#)]
74. Stupar, Y.V.; Schäfer, J.; García, M.G.; Schmidt, S.; Piovano, E.; Blanc, G.; Huneau, F.; Le Coustumer, P. Historical mercury trends recorded in sediments from the Laguna del Plata, Córdoba, Argentina. *Geochemistry* **2014**, *74*, 353–363. [[CrossRef](#)]
75. Veit, H. Southern Westerlies during the Holocene deduced from geomorphological and pedological studies in the Norte Chico, Northern Chile (27–33°S). *Palaeogeogr. Palaeoclim. Palaeoecol.* **1996**, *123*, 107–119. [[CrossRef](#)]
76. Link, O.; Brox-Escudero, L.M.; González, J.; Aguayo, M.; Torrejón, F.; Montalva, G.; Eguibar-Galán, M.Á. A paleo-hydro-geomorphological perspective on urban flood risk assessment. *Hydrol. Process.* **2019**, *33*, 3169–3183. [[CrossRef](#)]
77. Aronson, J.; Del Pozo, A.; Ovalle, C.; Avendaño, J.; Lavin, A.; Etienne, M. Land Use Changes and Conflicts in Central Chile. In *Landscape Disturbance and Biodiversity in Mediterranean-Type Ecosystems*; Rundel, P.W., Montenegro, R.G., Jaksic, F.M., Eds.; Ecological Studies: Berlin, Germany, 1998; pp. 155–168. [[CrossRef](#)]
78. Koch, A.; Brierley, C.; Maslin, M.M.; Lewis, S.L. Earth system impacts of the European arrival and Great Dying in the Americas after 1492. *Quat. Sci. Rev.* **2019**, *207*, 13–36. [[CrossRef](#)]
79. Cisternas, M.; Araneda, A.; Martínez, P.; Pérez, S. Effects of historical land use on sediment yield from a lacustrine watershed in central Chile. *Earth Surf. Process. Landf.* **2001**, *26*, 63–76. [[CrossRef](#)]
80. Basualto, S.; del Valle, J.; Gil, M.V.; Figueroa, R.; Parra, O.; Gonzalez, A.; Stehr, A. Modelos de gestión, conflictos y mediación en cuencas hidrográficas: Los casos de España y Brasil y su aplicabilidad a Chile. *Aqua-LAC* **2019**, *11*, 66–76. [[CrossRef](#)]